International Journal of Food Science +Technology

Institute of Food Science +Technology ifst

International Journal of Food Science and Technology 2020, **55**, 1637–1647

Original article

Application of ultrasound treatment for modulating the structural, functional and rheological properties of black bean protein isolates

Liang Li[1†] Yan Zhou[1†] Fei Teng,[1] Shuang Zhang,[1] Baokun Qi,[1] Changling Wu,[1] Tian Tian,[1] Zhongjiang Wang[1]* & Yang Li[1,2,3,4]*

1 College of Food Science, Northeast Agricultural University, Harbin 150030,China
2 Department of Food Science, Cornell University, Ithaca NY, 14853-7201,USA
3 Harbin Institute of Food Industry, Harbin 150030,China
4 Heilongjiang Academy of Green Food Science, Harbin 150030,China

(Received 28 July 2019; Accepted in revised form 22 October 2019)

Summary The modulating effect of ultrasound treatments at varying powers and times on the structural and functional properties of black bean protein isolate (BBPI) was investigated. Compared with native BBPI, low-power (150 W) and medium-power (300 W) ultrasound treatments increased the solubility, foaming and emulsifying properties of BBPI, especially at 300 W, 24 min. This effect arises predominantly due to increased exposure of hydrophobic groups, which serve to increase the interactions between the protein and water molecules. Additionally, an increase in the protein surface activity improved the absorption of protein molecules at the oil–water and air–water interfaces. Rheology data showed that increased hydrophobic and hydrogen-bonding interactions improved the water-holding capacity of BBPI gels following ultrasound treatment. However, high-power (450 W) ultrasound treatment weakened the functional properties of BBPI, and this was likely due to the formation of macromolecular BBPI aggregates. Overall, this study indicates that ultrasound treatment could be a promising approach for modulating other plant protein resources as well as expanding the application of black bean protein.

Keywords Black bean protein isolate, functional properties, protein molecular structural, rheology properties, ultrasound treatment.

Introduction

Black beans contain numerous high-quality proteins, with a higher content compared to that of soybeans, meat, eggs, milk and other resources. Black bean proteins are widely produced and processed for use in food products because of their high nutritional value and appropriate functional properties (He *et al.*, 2018). Black bean protein isolate (BBPI) is known for its high nutritional value, including an optimal balance of amino acids, abundant phytochemicals and specific nutrients, as well as possessing many biological functions, including anti-ageing and antioxidant. Nevertheless, the application of BBPI is restricted due to the incompatibility between its solubility and other properties such as emulsifying activity. As such, a number of approaches (e.g. physical, chemical and enzymatic modifications) have been employed to modify the structure and functional properties of these proteins. Currently, the most common methods for modifying the functional properties of BBPI are the Maillard reaction and enzymatic hydrolysis (Jing *et al.*, 2018; Xu *et al.*, 2018).

Adapting to developments in the contemporary food industry, ultrasound technology has attracted increasing attention as a green and reliable means of wide modifying food sources, including use in processing, quality control, extraction and modification of raw materials (Arzeni *et al.*, 2012). The most commonly used application is the use of low-power ultrasound (high frequency) as an analytical technique for analysing the physical and chemical properties of food, such as hardness, maturity, sweetness and acidity. High-power (low frequency) ultrasound is used to improve the physical and/or chemical properties of foods, mainly by way of cavitation, heating, vigorous agitation, shear force and turbulence. Cavitation is caused

*Correspondent: E-mails: wangzhongjiang@neau.edu.cn (Z.-J. Wang); yangli@neau.edu.cn (Y. Li)
†Liang Li and Yan Zhou contributed to the work equally and should be regarded as co-first authors.

doi:10.1111/ijfs.14428

© 2019 Institute of Food Science and Technology

by the rapid formation of bubbles and their intense collapse under ultrasound treatment, resulting in extreme temperatures, shear energy waves and turbulence effects in the cavitation zone (Soria & Villamiel, 2010). One attractive application of ultrasound technology is to help modulate the structure of proteins, thereby improving their functional properties, such as solubility (Jambrak *et al*., 2014). For bovine serum albumin (BSA) and ovalbumin (OVA), high-intensity ultrasound (HIUS) can decrease their interface tension (oil–water and air–water interface) and increase the emulsifying activity and foaming ability of these proteins, which results from the increase in surface activity and surface hydrophobicity (Gulseren *et al*., 2007; Xiong *et al*., 2016). The solubility and apparent viscosity of whey proteins are both significantly increased following treatment via ultrasound, and their flow behaviour altered to that of shear thickening (Jambrak *et al*., 2014). Therefore, ultrasound treatment represents an efficient and reliable method to improve the functional properties of plant proteins, and it also has the potential to help in the development of new products for use in the food industry.

Prior research has mainly focused on the potential effects of HIUS on the structural and functional properties of proteins. Studies on the effects of ultrasound power levels (low and medium) and times on the functional properties of proteins are limited, especially in regard to BBPI. In our previous research, changes in the structural properties and solubility of BBPI treated by ultrasound (power, 150, 300 and 450 W; time, 12 or 24 min) was assessed (Jiang *et al*., 2014); however, other functional properties were not fully investigated. In this current study, the impact of ultrasound treatment on the structural properties and free sulfhydryl content, as well as the solubility, foaming, emulsifying and gelation properties of BBPI, was assessed, with the aim of furthering our understanding of the relationship between the structural and functional properties of these proteins. The results of this study could help promote the application of BBPI in the food industry and might have significance in regard to utilising other plant protein resources.

Materials and methods

Materials

Defatted black bean powder (29.4% protein, 5.7% ash, 1.5% fat, 44.2% starch and 19.2% fibre) was obtained from Heilongjiang Agriculture Co., Ltd. (Harbin, Heilongjiang, China). To extract the black bean protein isolate (BBPI), defatted black bean powder (50.0 g) was dissolved in 500 mL of distilled water, and the pH was adjusted to 8.0 with NaOH (2 M). The mixture was extracted using alkaline, treated by magnetic stirring (3 h) and centrifuged (10 000 g, 4 °C, 30 min) to obtain a supernatant. The pH of the supernatant was then adjusted to 4.5 using 2 M HCl and centrifuged (10 000 g, 4 °C, 30 min) to obtain the precipitate. The precipitate was dialysed at 4 °C for 2 days, neutralised to 7.0 using NaOH (2 M) and freeze-dried. The Kjeldahl method (N × 5.8) was used to measure the content of protein in the final BBPI, and the content was determined to be 92.84%.

Ultrasound treatment

The dispersion (10%, w/v) was made by mixing BBPI power with distilled water in a 150-mL Erlenmeyer flask, which was then stirred constantly at 20 ± 2 °C for 2 h. Afterword, the dispersions were stored at 4 °C overnight. A JY92-IIN ultrasonic processor (Nanjing Karma Instrument Equipment Co., Ltd., Nanjing, China) equipped with a 0.636-cm-diameter titanium probe was used to treat the dispersion (100 mL) at a frequency of 20 kHz, and the temperature of the sample was maintained below 4 °C by immersion in an ice-water bath. BBPI was treated via ultrasound at different output powers (0, 150, 300 and 450 W) for 12 and 24 min (pulse duration: on-time, 4 s; off-time, 2 s). All treated samples were freeze-dried and stored in sealed containers.

Fourier-transform infrared (FT-IR) spectroscopy

The structure of the samples was analysed using an IRTracer-10 FT-IR spectrometer (Shimadzu Corporation, Kyoto, Japan) at 20 ± 2 °C. The BBPI samples (5 mg) and potassium bromide (295 mg) were mixed and compressed. The FT-IR spectra were recorded from 4000 to 400 cm^{-1}, with 64 scans at a 4 cm^{-1} resolution. The secondary structure was analysed using the 'Peakfit version 4.12' software, and 'Gaussian peak fitting' was the algorithm used.

Ultraviolet–visible (UV–Vis) spectra

A BBPI solution (0.5 mg mL^{-1}, w/v) was made by adding BBPI samples into 0.01 M phosphate-buffered solution (PBS) (pH 7.0). The UV–Vis spectra were recorded at 200-400 nm using a UV–Vis spectrophotometer (Shimadzu UV-2550) at 20 ± 2 °C with a 1.0 cm path length quartz cell. The scan rate and bandwidth were set at 60 nm min^{-1} and 2.0 nm, respectively. The PBS (0.01 M, pH 7.0) was used as a blank.

Determination of free sulfhydryl (-SH) content

Lyophilised samples were solubilised in pH 8.0 buffer (0.086 M Tris-0.09 M glycine, 4 mM Na_2EDTA) at a final protein concentration of 0.2%. The mixtures were incubated in a shaking water bath (24 h, 25 °C) and

© 2019 Institute of Food Science and Technology

then centrifuged (20 000 g, 4 °C) for 15 min to obtain the supernatant. The supernatant (5 mL) and Ellman's reagent solution (0.05 mL, 4 mg DTNB/mL buffer) were rapidly mixed and stand (20 °C, 15 min), and then measured at 340 nm. The buffer alone was used as a blank. A protein blank was used in which 0.03 mL of the buffer replaced the Ellman's reagent solution. A molar extinction coefficient of 1.36×104 M^{-1} cm^{-1} was used for calculating the micromoles of -SH/gram of protein.

Differential scanning calorimetry (DSC) measurements

The thermal stability of the BBPI samples was measured using a differential scanning calorimeter (TA Inc., New Castle, DE, USA). The BBPI samples (5 mg) were placed into an aluminium pan and then sealed tightly with an aluminium lid. The temperature programme increased from 20 °C to 110 °C at 10 °C/min under constant purging with dry nitrogen (50 mL min^{-1}) (Wan *et al.*, 2018). A sealed empty aluminium pan was used as a reference.

Determination of protein solubility

The pH of the lyophilised sample solution (200 mg L^{-1}) was adjusted to 7.0 using NaOH (2 M). This solution was stirred at 20 ± 2 °C for 1 h and then centrifuged (12 000 g, 20 min) using an Eppendorf 5430R centrifuge (Eppendorf AG, Hamburg, Germany). The Lowry method was used to determine the content of the supernatants. The ratio of the supernatant protein/total protein concentration before centrifugation was used as a measure of protein solubility (Zhu *et al.*, 2018).

Determination of emulsifying properties

The emulsion was prepared by homogenising 24 mL of BBPI solution (0.2%, w/v) with 8 mL of soybean oil at 13 500 r min^{-1} for 2 min. The emulsion (50 μL) was quickly withdrawn from the bottom (0 min) or after 10 min and added to 5 mL of a 0.1% sodium dodecyl sulphate (SDS) solution. The absorbance of the diluted emulsion was measured at 500 nm using a spectrophotometer, generating an emulsifying activity index (EAI) and emulsifying stability index (ESI) for the BBPI solution (Molina *et al.*, 2001). The EAI and ESI formulas were as follows:

$$\mathrm{EAI}\left(m^2/g\right) = 2T\frac{A_0 \times N}{C \times \theta \times \varphi \times 10000}$$

$$\mathrm{ESI}(\mathrm{min}) = \frac{A_0}{A_0 - A_{30}} \times 30.$$

where T is turbidity, N is the dilution factor, C is the initial concentration of protein (g mL^{-1}), θ is the length of the light path (1 cm), φ is oil fraction (0.2), and A_0 and A_{30} are the absorbance immediately (t = 0 min) and 30 min after emulsion formation, respectively.

Determination of foaming properties

The foaming capacity (FC) and foaming stability (FS) were observed for changes in the foam volume and liquid volume over time using an optical sensor (Duan *et al.*, 2018). A sample solution (100 mL, 0.2%, w/v) was placed in a 150-mL beaker and homogenised at a speed of 17 500 r/min for 40 s using a high-speed emulsifying homogeniser for 3 min. The volume of the foam immediately and 30 min after homogenisation was denoted as V_0 and V_{30}, respectively. The FC and FS formulas were as follows:

$$\mathrm{FC}(\%) = V_0/100 \times 100\%$$

$$\mathrm{FS}(\%) = V_{30}/V_0 \times 100\%$$

Preparation of BBPI gels

Lyophilised samples were dissolved in 50 mM PBS (pH 7.0) to a 10% (w/v) final concentration, and the pH was adjusted to 7.0. After stirring (2 h) at 20 ± 2 °C, the solution was heated (90 °C, 20 min), immediately cooled in an ice bath for 15 min and then stored at 4 °C for 24 h.

Gels strength and water-holding capacity (WHC)

WHC of BBPI gels and the calculated formulas were determined as described by Tang *et al.* (2009). A texture analyser (Universal TA; Shanghai Tengpu Instrument Technology Co., Ltd., Shanghai, China) was used to evaluate the gel strength at a speed of 1 mm s^{-1}.

Gel rheology

The rheology of the BBPI gels was evaluated using a Model AR1000 rheometer (TA Instruments, West Sussex, UK) with parallel plates (d = 27.83 mm); the gap between two plates was 1.0 mm. The BBPI sample solution (pH 7.0) was loaded onto the lower plate and dispersed with a spatula. The free edge of the sample was sealed by a thin layer of silicone oil to avoid moisture loss during the heating process. The heating–cooling cycle programme was set as: heating from 25 °C to 90 °C at 5 °C min^{-1}, holding at 90 °C for 30 min and cooling to 25 °C at the same speed. The storage modulus (G') and loss modulus (G'') were recorded as a

© 2019 Institute of Food Science and Technology

function of time during this process (Wu *et al*., 2011). The gels formed by temperature scanning were subjected to a frequency sweep (0.1–10.0 Hz) at 25 °C, and the fixed shape was changed to 0.01.

Statistical analysis

All of the experiments were carried out in triplicate, and the results were expressed as the mean ± the standard deviation. Means were compared using one-way analysis of variance (ANOVA) with a 95% confidence interval followed by Duncan's multiple range test. ANOVA results with $P < 0.05$ were considered statistically significant. Statistical analysis was performed using SPSS software version 19.0 (IBM, Armonk, New York, NY, USA).

Results

Characteristics of FT-IR spectra

Secondary structures are commonly analysed based on the amide I band (1700–1600 cm^{-1}), which is mainly derived from the C = O stretching vibration of the polypeptide backbone. The corresponding relationship between the sub-peaks and the secondary structure has been reported as: 1610–1640 cm^{-1} for β-sheet, 1640–1650 cm^{-1} for random coil, 1650–1660 cm^{-1} for α-helix and 1660–1700 cm^{-1} for β-turn (Zhang *et al*., 2003). In this study, the peak areas were calculated for the BBPI treated by different ultrasound conditions to determine the secondary structure contents (Table 1).

The FT-IR spectra of native and ultrasound-treated BBPI are depicted in Fig. 1a. The β-sheet was the predominant secondary structure of native BBPI, consistent with the data obtained via circular dichroism (CD) spectrum analysis (Jiang *et al*., 2014). The β-sheet content of the treated BBPI increased, and the proportion α-helix and random coil structures decreased (except for that treated at 450 W) compared to the native BBPI. This change might have arisen from a disruption of the stretching vibrations of amino acid sequences and intermolecular interactions between distinct parts of the protein molecules, thereby leading to changes in the protein conformation and a disordered molecular arrangement (Gulseren *et al*., 2007; Hu *et al*., 2013). The secondary structure of the ultrasound-treated BBPI presented a significant decrease in α-helix and random coil structures, and an increase in β-sheet following low-power (150 W) and medium-power (300 W) treatments. Longer treatment time can promote the expansion of protein chains, which would likely contribute to the occurrence of intermolecular interactions. However, high-power ultrasound and longer treatment time significantly increased the contents of α-helix and β-sheet structures in the treated BBPI, while reducing the contents of random coil structures. The increase in β-sheet structures in the treated BBPI was likely related to the formation of aggregates (Duan *et al*., 2018), as intermolecular β-sheet structures are commonly found in aggregated proteins (Lee *et al*., 2007). The cavitation effect and mechanical force generated via ultrasound could have accelerated the movement of the protein molecules and increased the possibility of molecular collision, leading to the formation of aggregates. A slight decrease in random coil structures in ultrasound-treated bovine serum albumin (20 kHz, 450W) has also been previously reported (Gulseren *et al*., 2007).

Characteristics of UV–Vis spectra

The UV–visible spectroscopy results for the native and ultrasound-treated BBPI are shown in Fig. 1b. The characteristic absorption at about 270 nm was mainly dependent on the absorption of phenylalanine, tyrosine and tryptophan (Huang *et al*., 2019). Ultrasound treatment increased the UV absorbance intensity at 270 nm, which might have been due to the unfolding of the protein molecules and subsequent exposure of hydrophobic groups. The redshift of the maximum absorbance wavelength of the ultrasound-treated BBPI

Table 1 Secondary structural content of native and ultrasound-treated black bean protein isolate (BBPI) estimated from FT-IR spectra at 25 °C

Samples	α-helix/%	β-sheet/%	β-turn/%	Random coil structures/%
BBPI (Control)	13.2 ± 0.1^{c}	42.9 ± 0.2^{c}	25.6 ± 0.2^{e}	18.3 ± 0.1^{a}
BBPI (150 W, 12 min)	12.5 ± 0.2^{d}	42.6 ± 0.2^{f}	27.2 ± 0.1^{c}	17.7 ± 0.2^{b}
BBPI (150 W, 24 min)	12.4 ± 0.2^{d}	43.8 ± 0.1^{c}	26.7 ± 0.0^{d}	17.1 ± 0.1^{d}
BBPI (300 W, 12 min)	11.4 ± 0.1^{f}	43.0 ± 0.2^{e}	28.2 ± 0.2^{a}	17.4 ± 0.0^{c}
BBPI (300 W, 24 min)	11.9 ± 0.1^{e}	43.5 ± 0.1^{d}	27.8 ± 0.2^{b}	16.8 ± 0.1^{e}
BBPI (450 W, 12 min)	15.0 ± 0.0^{b}	45.8 ± 0.2^{b}	22.5 ± 0.1^{f}	16.6 ± 0.2^{e}
BBPI (450 W, 24 min)	16.8 ± 0.1^{a}	49.2 ± 0.2^{a}	18.4 ± 0.1^{g}	15.6 ± 0.2^{f}

Different letters indicate significant differences between samples treated by different ultrasound conditions. The criterion for statistical significance was $P < 0.05$.

© 2019 Institute of Food Science and Technology

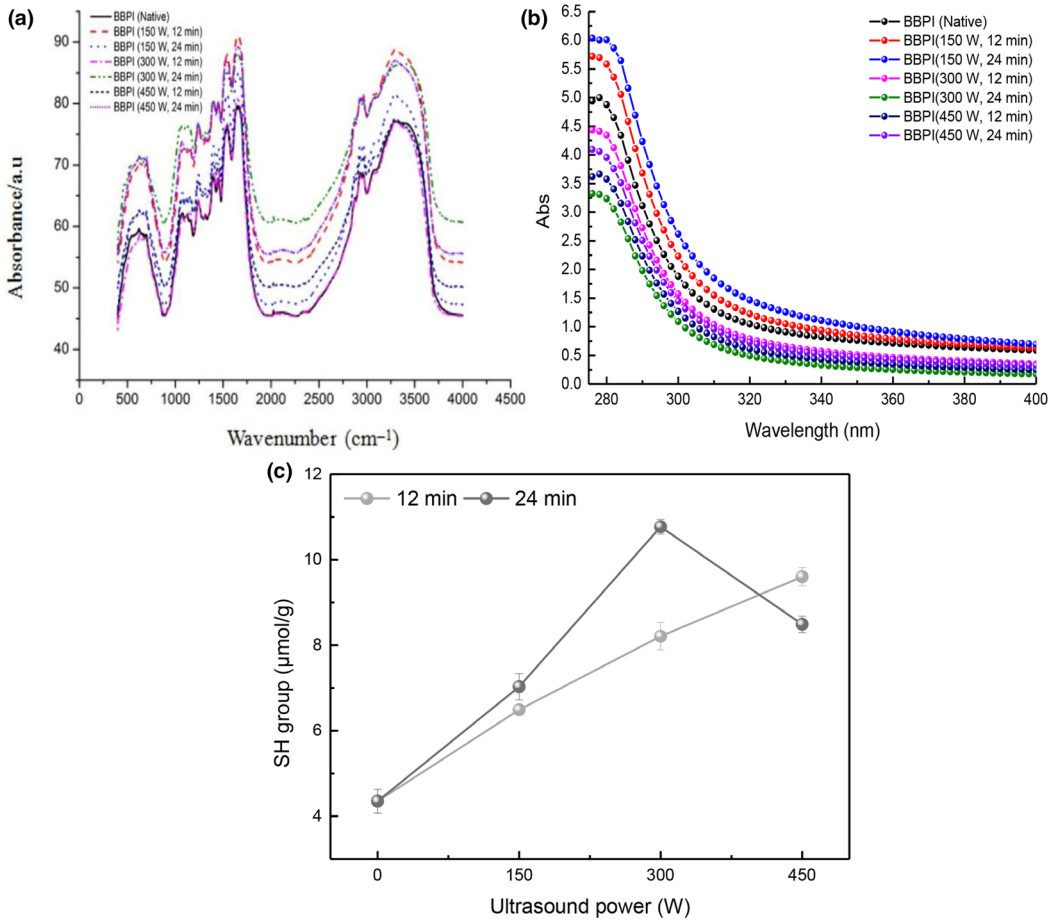

Figure 1 Structural properties of the native and treated BBPI subsequent to ultrasound treatment (powers: 150, 300 and 450 W; times: 12 and 24 min), (a): UV spectra of the native and treated BBPI at 0.5 mg mL^{-1}; (b): FT-IR spectra of the native and treated BBPI at 0.5 mg mL^{-1}; (c): content of free -SH groups in the native and treated BBPI subsequent to ultrasound treatment (powers: 150, 300 and 450 W; times: 12 and 24 min). [Colour figure can be viewed at wileyonlinelibrary.com]

likely indicated that interactions among the protein molecules were damaged, increasing the exposure of more hydrophobic groups (chromophores) (Huang *et al*., 2019). However, the absorption intensity of the ultrasound-treated BBPI was significantly decreased at an ultrasound power> 300 W, and this might have been due to the ultrasound treatment causing some hydrophobic groups to be embedded or the formation of large aggregates (Jin *et al*., 2015). Furthermore, the hydrogen-bonding and hydrophobic interactions of the ultrasound-treated sample treated at 450 W were not further reduction with the increase in treatment time (Hu *et al*., 2013).

Determination of free -SH groups

Free -SH groups are important functional moieties within proteins. The contents of free -SH groups can, thus, reflect the degree of denaturation of proteins and play an important role in their functional properties (e.g. solubility, emulsification and foaming ability). Figure 1c denotes that the free -SH group contents of the treated BBPI were significantly increased ($P < 0.05$). Ultrasound treatment induced the exposure of buried sulfhydryl groups to the surface of the protein molecules. High pressure, shear forces and cavitation effects can lead to a reduction in particle size, which further promotes the exposure of the sulfhydryl groups (Arzeni *et al*., 2012). The free -SH group contents of BBPI increased with treatment time during low- and medium-power ultrasound treatments (300 W, 24 min), from 4.35 ± 0.28 μmol g^{-1} to 10.77 ± 0.17 μmol g^{-1}. This increase could have arisen from the partial unfolding of the proteins, thereby exposing sulfhydryl groups to the surface (Fernandez-Diaz *et al*., 2000). Nevertheless, high-power ultrasound

© 2019 Institute of Food Science and Technology

treatment for an extended time decreased the content of free -SH groups in the treated BBPI sample. Under these conditions, the hydrogen peroxide produced via the cavitation effect might have oxidised susceptible free -SH groups, leading to a decrease in the free -SH group contents (Gulseren *et al*., 2007).

Thermal stability

The thermal denaturation temperature (Td) and denaturation enthalpy (ΔH) can provide information regarding the temperature at which protein denaturation occurs and the quantity of heat demanded to induce the denaturation, respectively (Kaushik *et al*., 2016). Table 2 indicates that native BBPI presented two typical endothermic peaks at 76.87 °C and 96.18 °C, corresponding to the Td values of β-conglycinin (7S) and globulin (11S), respectively. Ultrasound treatment significantly decreased the Td and ΔH of the treated BBPI relative to the native BBPI. A decline of the Td peak is related to changes in protein conformation and also to the amino acid composition. Additionally, a decrease in ΔH can result from breakage of intramolecular bonds within the protein molecules (Nazari *et al*., 2018). The Td of BPPI treated by low- and medium-power ultrasound was initially decreased but increased with time, which might be accounted for a decrease in protein conformational stability (Arzeni *et al*., 2012). However, the ΔH decreased as the treatment time increased during low- and medium-power ultrasound, and this decrease indicated that the unfolding of the ultrasound-treated BBPI required less energy (Nazari *et al*., 2018). Moreover, the Td and ΔH increased for the BBPI treated by high-power ultrasound, and this could be explained by the formation of protein aggregates via intermolecular hydrophobic interactions; likewise, the modified protein showed a more ordered and stable structure, which was consistent with the FT-IR results (Fig. 1a).

Solubility of BBPI

The solubility of the treated BBPI was significantly higher than that of the native BBPI, as shown in Fig. 2a. This change might have arisen from the breaking of internal interactions resulting in exposure of polar amino acids (hydrophilic amino acid residues) towards water (Xue *et al*., 2018). Another possible reason for this result could be a decrease in the particle size of BPPI due to hydrogen and hydrophobic bond breakage, subsequently increasing the hydration capacity between the protein and water molecules (Jiang *et al*., 2014; Nazari *et al*., 2018). The solubility of the ultrasound-treated BBPI significantly increased along with the treatment time at low and medium power. The mechanical shear forces and shockwaves generated by the ultrasound treatment damaged the interactions among the native aggregates BBPI and contributed to the formation of soluble proteins by enhancing the interaction between the protein and water molecules (Zhang *et al*., 2017). However, the solubility of the ultrasound-treated BBPI at high-power decreased along with the increasing treatment time. The formation of insoluble macromolecular BBPI aggregates via hydrogen bonds and hydrophobic interactions was likely the primary reason for this observed decrease in solubility (Hu *et al*., 2013).

Emulsifying properties of BBPI

Figure 2b illustrates the EAI and ESI of the native and treated BBPI. The EAI and ESI represent the ability of proteins to adsorb at the oil–water interface during emulsion formation and the ability of proteins to maintain a two-phase stability, respectively (Chen *et al*., 2013). Compared to the native protein, the EAI and ESI of the treated BBPI were significantly increased, and this was likely due to the change in protein conformation increasing the surface-to-volume ratio, leading to more protein participating in

Table 2 Thermal properties of native and ultrasound-treated BBPI in 150, 300 and 450 W for 12 and 24 min

	7S		11S	
Samples	**Td (°C)**	**ΔH (J g^{-1})**	**Td (°C)**	**ΔH (J g^{-1})**
BBPI (Native)	76.87 ± 0.05^{a}	1.296 ± 0.03^{a}	96.18 ± 0.15^{a}	8.441 ± 0.12^{a}
BBPI (150 W, 12 min)	74.29 ± 0.44^{d}	0.999 ± 0.01^{b}	95.22 ± 0.11^{b}	8.073 ± 0.05^{b}
BBPI (150 W, 24 min)	73.34 ± 0.57^{e}	0.669 ± 0.04^{c}	93.01 ± 0.14^{d}	7.625 ± 0.14^{d}
BBPI (300 W, 12 min)	74.17 ± 0.26^{d}	0.443 ± 0.01^{f}	94.52 ± 0.28^{c}	6.823 ± 0.17^{d}
BBPI (300 W, 24 min)	73.23 ± 0.27^{e}	0.421 ± 0.02^{g}	94.24 ± 0.13^{c}	6.232 ± 0.21^{f}
BBPI (450 W, 12 min)	76.21 ± 0.15^{c}	0.621 ± 0.03^{d}	96.32 ± 0.22^{a}	7.985 ± 0.07^{c}
BBPI (450 W, 24 min)	76.55 ± 0.11^{b}	0.541 ± 0.09^{e}	96.16 ± 0.12^{a}	7.367 ± 0.19^{e}

Different letters indicate significant differences between samples treated by different ultrasound conditions. The criterion for statistical significance was $P < 0.05$.

© 2019 Institute of Food Science and Technology

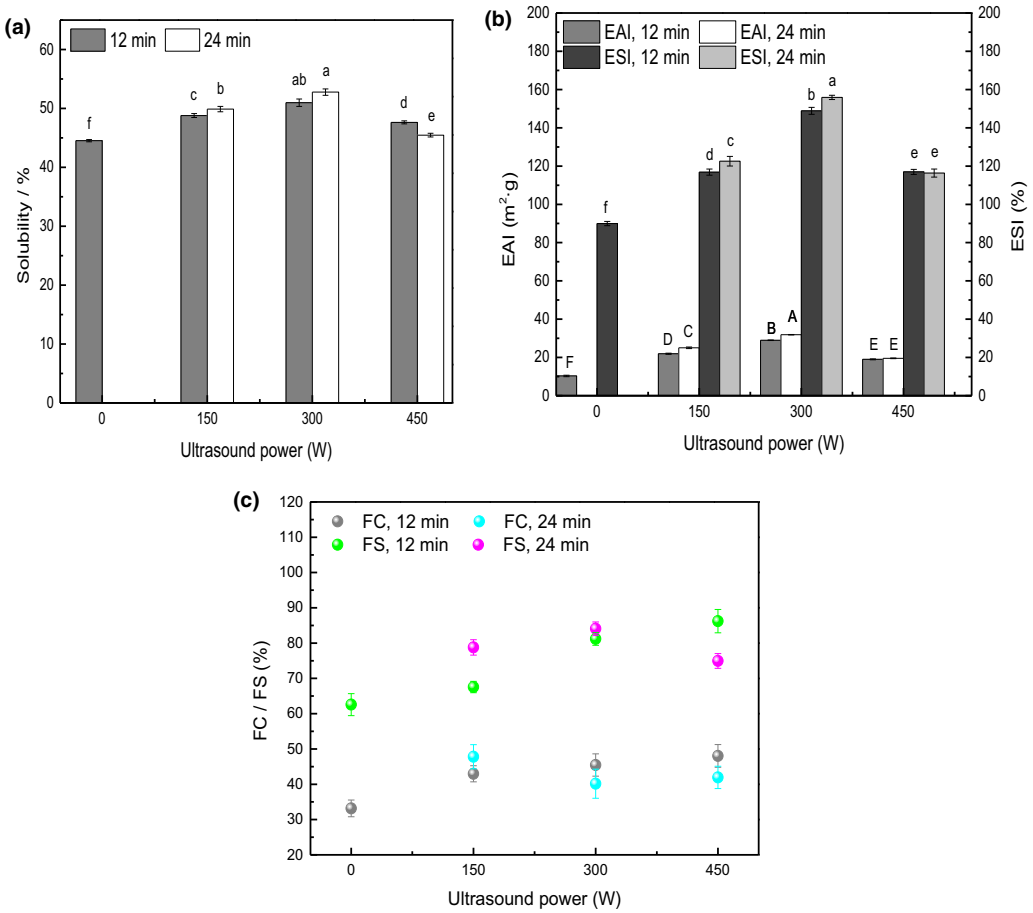

Figure 2 Functional properties of the native and treated BBPI subsequent to ultrasound treatment (powers: 150, 300 and 450 W; times: 12 and 24 min); (a): solubility; (b): emulsifying properties; (c): foaming properties. [Colour figure can be viewed at wileyonlinelibrary.com]

interfacial layer formation and an increased emulsifying efficiency. The EAI and ESI of the treated BBPI at low and medium power were both significantly increased along with the treatment time. The main reason for this result was likely due to the partial unfolding of the protein molecules and the subsequent increase of the surface activity of these proteins, allowing them to spread at the water–oil interface rapidly. Previously, Wang *et al.* (2008) demonstrated that the acoustic cavitation effect can change the conformation of protein, exposing more hydrophobic groups to the surface of the proteins, which could give rise to an increase in the EAI. The increase in the ESI has been attributed to conformational changes in the protein molecule promoting a more favourable orientation of the proteins (Amiri *et al.*, 2018). However, treatment with high-power ultrasound decreased the EAI and ESI of the treated BBPI, and this was independent of the treatment time. High pressure and cavitation effects have been shown to accelerate the interaction of intermolecular disulphide bonds and increase the formation of protein aggregates, resulting in reduced protein emulsifying properties (Molina *et al.*, 2001). Moreover, Yang *et al.* (2017) confirmed that the emulsifying properties were related to the solubility of the protein in solution.

Foaming properties of BBPI

The formation of foam is related to the surface hydrophobicity and structural flexibility of the proteins (Amiri *et al.*, 2018). Figure 2c demonstrates that ultrasound treatment significantly increased the FC and FS of the treated BBPI compared to the native BBPI, and this result might be related to the exposure of hydrophobic regions and a reduction of interfacial tension via unfolding of the BBPI molecules, which would be consistent with the FT-IR data (Fig. 1a). Additionally, higher levels of hydrophobicity could improve the foaming properties. The FC and FS of the treated

© 2019 Institute of Food Science and Technology

BBPI solutions monotonically increased with the increasing treatment power. Higher ultrasound powers caused more buried hydrophobic regions to be exposed from the interior of the molecules via the cavitation effect (Chen *et al*., 2012). The FC and FS of the ultrasound-treated BBPI were increased at low power and further increased with treatment time. A prolonger treated time further induced the unfolding of BBPI and subsequently increased the FC (Jambrak *et al*., 2008). It is worth noting that, although the medium- and high-power ultrasound treatment increased the FC of BBPI, this effect decreased with the increase in treatment time. We speculated that most of the BPPI molecules were desorbed from the gas–liquid interface and readily interacted with other desorbed molecules to form aggregates via covalent interactions, leading to an increase in the FC (Wang *et al*., 2019). The FS of the BBPI treated with medium-power ultrasound increased along with the treatment time. As more hydrophobic groups and regions were exposed to the liquid surface, the possibility of forming soluble protein aggregates was increased, and the gas–liquid boundary area was also increased, resulting in an increased FS (Xiong *et al*., 2018). The FS of the BBPI treated with high-power ultrasound increased, but the FS decreased with increasing treatment time. This decrease in the FS might have been related to the large amount of aggregated protein molecules and severe denaturation of the protein over the longer treatment time. Prior research has indicated that denaturation of proteins can lead to a decrease in the FC and FS (Jung *et al*., 2006).

WHC and the strength of BBPI gels

Table 3 shows that the WHC and gel strength of the treated BBPI were significantly increased compared to the native BBPI. It appeared that ultrasound treatment could facilitate the formation of a dense and uniform gel network that could hold more water (Shen *et al*., 2017). The content of free -SH groups played a prevailing role in the enhancement of the whey protein isolate (WPI) gels strength, which was confirmed by the above-mentioned data (Alting *et al*., 2003). Moreover, Madadlou *et al*. (2009) suggested that extensive inter-particle connections and rearrangements could promote the formation of dense gels. The WHC and gel strength of the ultrasound-treated BBPI increased following low- and medium-power ultrasound treatments, which was likely due to the smaller particle size and the increase in interactions among the BBPI molecules within the gel network. The unfolded polypeptide chains would increase the exposure of hydrophobic amino acid groups, thus contributing to the gel strength (Tan *et al*., 2014). However, high-power ultrasound treatment decreased the WHC and gel strength of the treated BBPI independent of the treatment time, and this might have been due to the formation of aggregates via hydrophobic interactions among the denatured BBPI protein molecules.

Gel rheology of BBPI

Rheology properties

Figure 3a displays the phase angle and G' of the native and ultrasound-treated BBPI. For all samples, G' was divided into three stages. The G' of the native and treated BBPI gels decreased during the initial heating process, indicating the gel networks might not have been completely formed. During the later heating process, the G' of treated BBPI gels sharply increased, and this was probably due to the ultrasound treatment inducing opening of the protein chain and, subsequently, improving the formation of junction zones via hydrogen bonding (Amiri *et al*., 2018). During the holding period (90 °C, 20 min), a significant increase in the strength of the gels was observed, and the network transformed from a viscous sol to elastic gel. The exposure of more buried hydrophobic groups and increased amount of bonds between the protein chains favour a stronger gel formation (Joshi *et al*., 2011). The gel strength of the treated BBPI was further strengthened as the temperature was reduced from 90 to 25 °C, and further enhancement of the colloidal network was evident upon cooling. It appeared that the interaction became stronger between protein chains

Table 3 Impact of different powers (0, 150, 300 and 450 W) and duration (12 and 24 min) of ultrasound treatment on BBPI solubility and gel strength

	Water-holding capacity (%)			Gel strength (g)		
Ultrasound time (min)	**150 W**	**300 W**	**450 W**	**150 W**	**300 W**	**450 W**
0	65.11 ± 0.12^{b}	65.11 ± 0.12^{b}	65.11 ± 0.12^{b}	28.02 ± 0.01^{c}	28.02 ± 0.01^{c}	28.02 ± 0.01^{c}
12	71.84 ± 0.04^{a}	75.03 ± 0.19^{a}	68.36 ± 0.22^{a}	35.07 ± 0.03^{b}	45.06 ± 0.07^{b}	49.90 ± 0.09^{b}
24	72.05 ± 0.07^{a}	75.58 ± 0.31^{a}	68.85 ± 0.17^{a}	36.89 ± 0.04^{a}	55.03 ± 0.01^{a}	52.72 ± 0.11^{a}

Different letters indicate significant differences between samples treated by different ultrasound conditions. The criterion for statistical significance was $P < 0.05$.

© 2019 Institute of Food Science and Technology

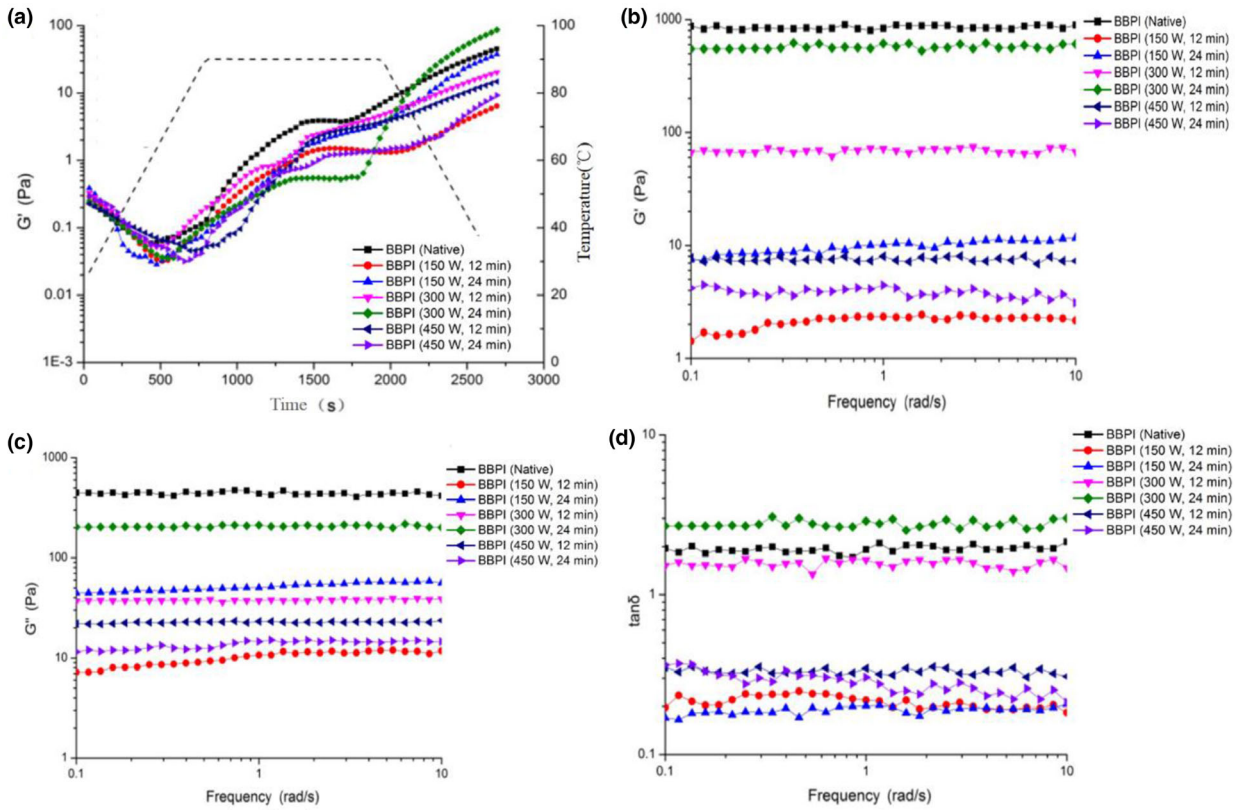

Figure 3 Influence of different ultrasound powers and times on the rheological properties of BBPI. Gel-frequency sweep: comparison of G′ versus frequency for BBPI after 12- or 24-min ultrasound treatment at power of 150, 300 and 450 W from the linear viscoelastic region during heating and cooling (a). Influence of the different ultrasonic treatments on the variation of the storage modulus (G') (b), loss modulus (G") (c) and phase angle (δ) (d) of BBPI. [Colour figure can be viewed at wileyonlinelibrary.com]

with the decrease in temperature, especially at the final stage, and this might be attributed to non-covalent interactions among the denatured BBPI protein molecules (Sun *et al*., 2011).

Frequency sweep analyses

G' is the energy stored by the gels during the deformation process due to elastic deformation, and it represents the firmness of the gel, which depends on the number of interactions and the binding energy between the protein chains (Amiri *et al*., 2018). G" is the energy that the gels lose in the form of heat due to viscous deformation during deformation. The phase angle (δ) is equal to the arc tangent of the G" to the G', which represents the viscous or elastic behaviour of gels. Figure 3b-d shows the influence of the different ultrasound powers and times on G', G" and δ of both native and treated BBPI. The G' of the treated BBPI was higher than the G", indicating that ultrasound treatment augmented the strength of the gels formed from treated BBPI. This might have been a result of the unfolding of proteins due to ultrasound treatment and subsequent formation of new inter- and intramolecular interactions (Frydenberg *et al*., 2016). Furthermore, the formation of higher-strength BBPI gels might also be related to an increase in the proportion of β-sheet structures, as demonstrated by Malik & Saini (2017) and Shevkani *et al*. (2015). Moreover, the increased solubility of the BBPI solution was another important factor likely influencing the formation of stronger gels (Malik & Saini, 2018).

Conclusions

Compared with the native BBPI, low- and medium-power ultrasound treatments caused the opening of the protein chain and exposure of buried hydrophobic groups, increasing the interaction between the protein and water molecules, which was highly beneficial to solubility. The exposure of hydrophobic groups led to

© 2019 Institute of Food Science and Technology

more efficient absorption of the protein molecules at the oil–water and air–water interfaces, improving the emulsifying and foaming properties of the BBPI. The decrease in particle size and increase in the interactions among hydrophobic groups were important factors affecting the formation of high-water-capacity gels. The DSC data indicated that the ΔH of the ultrasound-treated BBPI declined compared to the native BBPI, which was likely due to the destruction of intramolecular bonds. The formation of aggregates was the primary trend following protein conformational changes induced by the high-power ultrasonic treatment. As the content of ordered structure increases, the particle size also increases, which has a negative effect on emulsifying and foaming properties. Ultrasound technology can be used as an environmentally friendly method to improve the functional properties of proteins and meet the complex needs of modern food products; however, the effects of aggregate formation following high-power ultrasound treatment of BBPI in relation to the functional properties of the proteins still require further study.

Acknowledgments

This research was funded by the National Natural Science Foundation of China (2018YFD040050302 and 31571876); Heilongjiang Province General Undergraduate Higher Education Youth Innovative Talents Training Programme (NYPYSCT-2018163); Heilongjiang Provincial Science Foundation Project (C2018024); China Postdoctoral Science Foundation Funded Project (2018M641798); and Heilongjiang Province Postdoctoral Science Foundation Funded Project (LBH-Z18030).

Data availability statement

The data that support the findings of this study are openly available in [repository name, for example 'figshare'] at http://doi.org/[doi], reference number [reference number].

Ethical approval

Ethics approval was not required for this research.

Conflict of interest

The authors confirm that this manuscript has no conflicts of interests.

References

Alting, A.C., Hamer, R.J., de Kruif, C.G., Paques, M. & Visschers, R.W. (2003). Number of thiol groups rather than the size of the aggregates determines the hardness of cold set whey protein gels. *Food Hydrocolloids*, **17**, 469–479.

Amiri, A., Sharifian, P. & Soltanizadeh, N. (2018). Application of ultrasound treatment for improving the physicochemical, functional and rheological properties of myofibrillar proteins. *International Journal of Biological Macromolecules*, **111**, 139–147.

Arzeni, C., Martínez, K., Zema, P., Arias, A., Pérez, O.E. & Pilosof, A.M.R. (2012). Comparative study of high intensity ultrasound effects on food proteins functionality. *Journal of Food Engineering*, **108**, 463–472.

Chen, L., Chen, J.S., Yu, L., Wu, K.G., Liu, X.L. & Chai, X.H. (2012). Modifications of Soy Protein Isolates Using Ultrasound Treatment for Improved Emulsifying Properties. *Advanced Materials Research*, **554–556**, 944–948.

Chen, N., Zhao, M., Sun, W., Ren, J. & Cui, C. (2013). Effect of oxidation on the emulsifying properties of soy protein isolate. *Food Research International*, **52**, 26–32.

Duan, X., Li, M., Shao, J. *et al*. (2018). Effect of oxidative modification on structural and foaming properties of egg white protein. *Food Hydrocolloids*, **75**, 223–228.

Fernandez-Diaz, M.D., Barsotti, L., Dumay, E. & Cheftel, J.C. (2000). Effects of pulsed electric fields on ovalbumin solutions and dialyzed egg white. *Journal of Agricultural & Food Chemistry*, **48**, 2332–2339.

Frydenberg, R.P., Hammershoj, M., Andersen, U., Greve, M.T. & Wiking, L. (2016). Protein denaturation of whey protein isolates (WPIs) induced by high intensity ultrasound during heat gelation. *Food Chemistry*, **192**, 415–423.

Gulseren, I., Guzey, D., Bruce, B.D. & Weiss, J. (2007). Structural and functional changes in ultrasonicated bovine serum albumin solutions. *Ultrasonics Sonochemistry*, **14**, 173–183.

He, Q., Sun, X., He, S. *et al*. (2018). PEGylation of black kidney bean (*Phaseolus vulgaris* L.) protein isolate with potential functironal properties. *Colloids Surf B Biointerfaces*, **164**, 89–97.

Hu, H., Wu, J., Li-Chan, E.C.Y. *et al*. (2013). Effects of ultrasound on structural and physical properties of soy protein isolate (SPI) dispersions. *Food Hydrocolloids*, **30**, 647–655.

Huang, L., Ding, X., Li, Y. & Ma, H. (2019). The aggregation, structures and emulsifying properties of soybean protein isolate induced by ultrasound and acid. *Food Chemistry*, **279**, 114–119.

Jambrak, A.R., Mason, T.J., Lelas, V., Herceg, Z. & Herceg, I.L. (2008). Effect of ultrasound treatment on solubility and foaming properties of whey protein suspensions. *Journal of Food Engineering*, **86**, 281–287.

Jambrak, A.R., Mason, T.J., Lelas, V., Paniwnyk, L. & Herceg, Z. (2014). Effect of ultrasound treatment on particle size and molecular weight of whey proteins. *Journal of Food Engineering*, **121**, 15–23.

Jiang, L., Wang, J., Li, Y. *et al*. (2014). Effects of ultrasound on the structure and physical properties of black bean protein isolates. *Food Research International*, **62**, 595–601.

Jin, J., Ma, H., Wang, K. *et al*. (2015). Effects of multi-frequency power ultrasound on the enzymolysis and structural characteristics of corn gluten meal. *Ultrasonics Sonochemistry*, **24**, 55–64.

Jing, X., Dong, H., Chen, Z., Meng, L. & Hua, J. (2018). Effect of glucose glycosylation following limited enzymatic hydrolysis on functional and conformational properties of black bean protein isolate. *European Food Research and Technology*, **244**, 1111–1120.

Joshi, M., Adhikari, B., Aldred, P., Panozzo, J.F. & Kasapis, S. (2011). Physicochemical and functional properties of lentil protein isolates prepared by different drying methods. *Food Chemistry*, **129**, 1513–1522.

Jung, S., Murphy, P.A. & Johnson, L.A. (2006). Physicochemical and functional properties of soy protein substrates modified by low levels of protease hydrolysis. *Journal of Food Science*, **70**, 180–187.

Kaushik, P., Dowling, K., McKnight, S., Barrow, C.J., Wang, B. & Adhikari, B. (2016). Preparation, characterization and functional

© 2019 Institute of Food Science and Technology

properties of flax seed protein isolate. *Food Chemistry*, **197**(Pt A), 212–220.
Lee, S.H., Lefèvre, Thiery, Subirade, M. & Paquin, P. (2007). Changes and roles of secondary structures of whey protein for the formation of protein membrane at soy oil/water interface under high-pressure homogenization. *Journal of Agricultural and Food Chemistry*, **55**, 10924–10931.
Madadlou, A., Emam-Djomeh, Z., Mousavi, M.E., Mohamadifar, M. & Ehsani, M. (2009). Acid-induced gelation behavior of sonicated casein solutions. *Ultrasonics Sonochemistry*, **17**, 153–158.
Malik, M.A. & Saini, C.S. (2017). Polyphenol removal from sunflower seed and kernel: Effect on functional and rheological properties of protein isolates. *Food Hydrocolloids*, **63**, 705–715.
Malik, M.A. & Saini, C.S. (2018). Rheological and structural properties of protein isolates extracted from dephenolized sunflower meal: Effect of high intensity ultrasound. *Food Hydrocolloids*, **81**, 229–241.
Molina, E., Papadopoulou, A. & Ledward, D. (2001). Emulsifying properties of high pressure treated soy protein isolate and 7S and 11S globulins. *Food Hydrocolloids*, **15**, 263–269.
Nazari, B., Mohammadifar, M.A., Shojaee-Aliabadi, S., Feizollahi, E. & Mirmoghtadaie, L. (2018). Effect of ultrasound treatments on functional properties and structure of millet protein concentrate. *Ultrasonics Sonochemistry*, **41**, 382–388.
Shen, X., Zhao, C. & Guo, M. (2017). Effects of high intensity ultrasound on acid-induced gelation properties of whey protein gel. *Ultrasonics Sonochemistry*, **39**, 810–815.
Shevkani, K., Singh, N., Kaur, A. & Rana, J.C. (2015). Structural and functional characterization of kidney bean and field pea protein isolates: A comparative study. *Food Hydrocolloids*, **43**, 679–689.
Soria, A.C. & Villamiel, M. (2010). Effect of ultrasound on the technological properties and bioactivity of food: a review. *Trends in Food Science & Technology*, **21**, 323–331.
Sun, W.-W., Yu, S.-J., Yang, X.-Q. *et al*. (2011). Study on the rheological properties of heat-induced whey protein isolate–dextran conjugate gel. *Food Research International*, **44**, 3259–3263.
Tan, M.C., Chin, N.L., Yusof, Y.A., Taip, F.S. & Abdullah, J. (2014). Gel strength and stability characterization of ultrasound treated whey protein foams. *Agriculture and Agricultural Science Procedia*, **2**, 144–149.
Tang, C.-H., Wang, X.-Y., Yang, X.-Q. & Li, L. (2009). Formation of soluble aggregates from insoluble commercial soy protein isolate by means of ultrasonic treatment and their gelling properties. *Journal of Food Engineering*, **92**, 432–437.
Wan, Y., Liu, J. & Guo, S. (2018). Effects of succinylation on the structure and thermal aggregation of soy protein isolate. *Food Chemistry*, **245**, 542–550.
Wang, X.-S., Tang, C.-H., Li, B.-S., Yang, X.-Q., Li, L. & Ma, C.-Y. (2008). Effects of high-pressure treatment on some physicochemical and functional properties of soy protein isolates. *Food Hydrocolloids*, **22**, 560–567.
Wang, M.-P., Chen, X.-W., Guo, J., Yang, J., Wang, J.-M. & Yang, X.-Q. (2019). Stabilization of foam and emulsion by subcritical water-treated soy protein: Effect of aggregation state. *Food Hydrocolloids*, **87**, 619–628.
Wu, M., Xiong, Y.L. & Chen, J. (2011). Rheology and microstructure of myofibrillar protein–plant lipid composite gels: Effect of emulsion droplet size and membrane type. *Journal of Food Engineering*, **106**, 318–324.
Xiong, W., Wang, Y., Zhang, C. *et al*. (2016). High intensity ultrasound modified ovalbumin: Structure, interface and gelation properties. *Ultrasonics Sonochemistry*, **31**, 302–309.
Xiong, T., Xiong, W., Ge, M., Xia, J., Li, B. & Chen, Y. (2018). Effect of high intensity ultrasound on structure and foaming properties of pea protein isolate. *Food Research International*, **109**, 260–267.
Xu, X.Y., Yong, C., Hao, Z. *et al*. (2018). Effects of corn starch on the gel properties of black bean protein isolate. *Journal of Texture Studies*, **49**, 548–555.
Xue, F., Zhu, C., Liu, F., Wang, S., Liu, H. & Li, C. (2018). Effects of high-intensity ultrasound treatment on functional properties of plum (Pruni domesticae semen) seed protein isolate. *Journal of the Science of Food and Agriculture*, **98**, 5690–5699.
Yang, W.H., Tu, Z.C., Wang, H., Li, X. & Tian, M. (2017). High-intensity ultrasound enhances the immunoglobulin (Ig)G and IgE binding of ovalbumin. *Journal of the Science of Food and Agriculture*, **97**, 2714–2720.
Zhang, X., Huang, L.X., Nie, S.-Q., Qi, X.-R. & Zhang, Q. (2003). FTIR characterization of the secondary structure of insulin encapsulated within liposome. *Journal of Chinese Pharmaceutical Sciences*, **12**, 11–14.
Zhang, Z., Regenstein, J.M., Zhou, P. & Yang, Y. (2017). Effects of high intensity ultrasound modification on physicochemical property and water in myofibrillar protein gel. *Ultrasonics Sonochemistry*, **34**, 960–967.
Zhu, Z., Zhu, W., Yi, J. *et al*. (2018). Effects of sonication on the physicochemical and functional properties of walnut protein isolate. *Food Research International*, **106**, 853–861.

© 2019 Institute of Food Science and Technology